Modeling of Ultrasonic Testing in Butt Joint by Ray Tracing

Young-Hyun Nam*
R&D Center, Hanjung

Ultrasonic wave generation and propagation were modeled to simulate an ultrasonic test. A ray model was used for the modeling. Actual sound pressure distribution of the incident wave from an angle probe was analyzed using an ultrasonic visualization method to incorporate the actual sound pressure distribution in the model. In this method, the sound pressure was expressed by the density of rays and the reflection coefficient of ultrasonic beams. Reflection and mode conversion of rays were computed by the Snell's law. Simulation programs for the problem of ultrasonic testing of a butt joint are built using this ray modeling. Simulation results for ultrasonic wave scattering from a defect and A-scan display in ultrasonic testing agreed with the actual experiment results.

Key Words : Ultrasonic Testing, Visualization, Butt Joint, Ray Tracing

1. Introduction

Ultrasonic testing utilizes the echoes from defects. Spurious echoes, which are not from flaws, appear on the A-scan display because of the mode conversion during the propagation in the complex shape of specimen. It is necessary to understand ultrasonic wave propagation for reliable ultrasonic testing of materials of general shape.

For this purpose, visualization method has been applied to comprehend wave propagation and scattering at any defects which may exist (Baborovsky et al, 1973; Harker, 1984; Nam, 1999; Serabian, 1982). Computer simulation analyses of wave propagation have also been conducted. A particles model (Harumi, 1986; Harumi and Uchida, 1990; Harumi et al, 1992) and an iterative ray tracing model (Ogilvy and Temple, 1983; Ogilvy; 1984, 1985, 1986, 1987, 1988, 1992) were applied for such simulations. However, these were mostly concerned with fundamental wave scattering phenomena at the defects, or with beam propagation.

This paper presents a simple simulation model that can predict the actual ultrasonic testing signals. This ray model simulates the propagation of ultrasonic waves in a specimen and can be used to predict the echo position in an A-scan display. The actual sound pressure distribution of a generated wave was analyzed by using a visualization system to incorporate the sound pressure distribution into the model. A group of rays corresponded to the ultrasonic beam, and sound pressure was expressed as the density of rays. The change of sound pressure at reflection was calculated for all rays using the reflection coefficients. The direction of each reflected wave was calculated using the Snell's law. Simulation programs for ultrasonic testing of a butt joint were developed using this ray modeling. Typical simulation results for the scattering of ultrasonic waves from a defect agreed with the experimental results obtained by an ultrasonic visualization method.

* **E-mail** : namyh@hanjung.com
TEL : +82-55-278-3776; **FAX** : +82-55-278-8546
R & D center, Hanjung, 555 Guygok-dong, Changwon, Kyungnam 641-792, Korea.(Manuscript **Received** July 31, 2000; **Revised** January 15, 2001)

2. Observation of Ultrasonic Waves

The visualization system (Nam, 1999) is based on a synthesized photoelastic method for a sound

pressure analysis of waves. The system consists of a regular linear polariscope with a commercial stroboscopic light source and a digital image-processing system. The trigger pulse actuating the stroboscope has a delay time relative to the trigger pulse of the ultrasonic flaw detector, and by varying this delay time an observer can change the position at which the pulsed ultrasound is stroboscopically frozen and imaged. A CCD camera is used to visualize the ultrasonic wave in a solid. The image is divided into 512 lines, and each line is divided into 512 parts. The brightness is converted into a video signal with 8-bit resolution. The amplitude (brightness) of the ultrasonic wave is represented in polar coordinates (r, θ), using the values of 128 and 256 in terms of a directivity mean of 0.25 and 0.5 V, respectively, in the visualized image. Angle probes with 4 MHz frequency and 60° nominal refraction angle for steel were used. Machine oil was used as the acoustic couplant.

The directivity was almost constant during the propagation. Actual refraction angle of this probe was 65 degrees, due to the velocity difference between steel and pyrex glass used in this experiment. The beam pattern was symmetric with respect to the 65 degrees direction. The range of angle over which the sound pressure has decreased down to 50 percent of the maximum pressure (-6dB) was 65±5.5 degrees. Sound pressure (P) relative to the radiation angle from 65 degrees could be expressed as follows:

$$P=100-2.46\phi-0.526\phi^2 \quad (1)$$

where P is the relative sound pressure and

$$\phi=|\,(\text{radiation angle})-65\ \text{degrees}\,| \quad (2)$$

Equation (1) is obtained by fitting, at interval of 1 degree, the sound pressure of shear wave emitted from the angle probe, measured by using the visualization method.

3. Directivity

The directivity of ultrasonic waves is closely related to the testing sensitivity, the scanning pitch, the arrangement of probes, and the defect

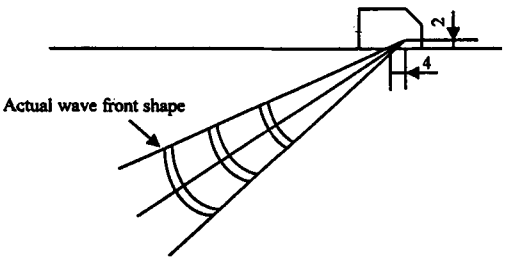

Fig. 1 Schematic diagram of ultrasonic wave from angle probe

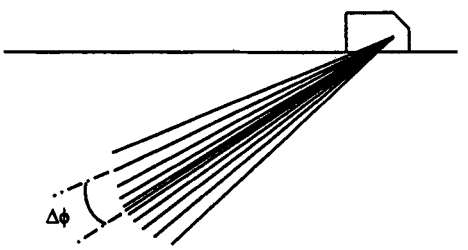

Fig. 2 Schematic diagram of sound pressure distribution

size and location. The directivities of ultrasonic waves were obtained from the relationship between the angle and the maximum sound pressure value. The shape of the wavefront is spherical and the point source of the wave, or the central point of this spherical wavefront, was located inside an angle probe as shown in Fig. 1. The directivity of sound pressure from this central point was analyzed by the visualized image, in which the intensity of the visualized image was correlated with the absolute sound pressure of the wave.

4. Modeling of Ultrasonic Wave Generation

Since the ultrasonic wave was generated from the point source as shown in Fig. 1, we made a simple model for the ultrasonic wave generation from the angle probe, shown schematically in Fig. 2. A group of rays represents the ultrasonic beam. Each ray direction shows a wave propagating direction. The rays are generated from the point source radially within the 65±5.5 degrees range. In order to illustrate the angular distribution of sound pressure, we changed the line spacing

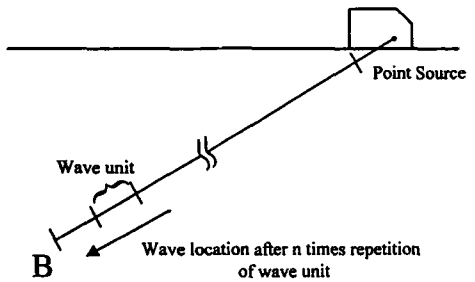

Fig. 3 Schematic diagram of wave propagation

within the ultrasonic beam. In the ray modeling, a decrease of sound pressure was expressed as an increase in the angular distance between the neighboring rays. The angle increase was determined from the actual sound pressure distribution of Eq. (1) by the following equation:

$$\Delta\phi = 5.5(2 - P/50) \tag{3}$$

where $\Delta\phi$ is the absolute angle increase; $P = 100 - 2.46X - 0.526X^2$; $X = 5.5(i-1)/(N-1)$; $2N-1$ is the total number of the ray; and i is any integer between 1 and N.

Calculations for wave propagation were carried out as shown in Fig. 3: a small wave unit that starts from the point source was extended repeatedly along the defined direction of the ray. The wave propagates to point B after n times of repetition, as shown in Fig. 3. The length of this wave unit is proportional to the wave velocity. Then the beam path distance can be calculated from the wave unit length and its repetition time. This small wave unit includes the information of the wave propagation direction, wave velocity, beam path distance, and sound pressure. The small wave units on all rays in Fig. 2 are similarly extended as the waves propagate.

Simulated ultrasonic wave generation using this ray modeling is presented in Fig. 4. Figure 4 (a) is the wave front, showing the wave units at the same time steps from the point source. Sound pressure distribution of the simulated wave is shown in Fig. 4(b). This distribution was calculated from the number of wave units contained within every 1 degree range. This result agrees well with the experimental results analyzed by the visualization method.

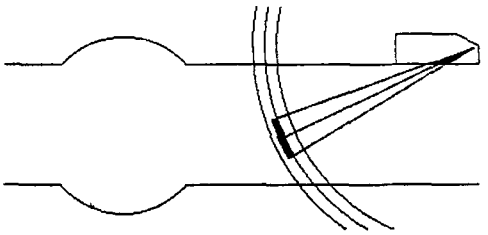

(a) Wave front shape

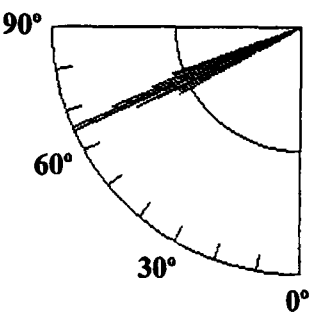

(b) Directivity

Fig. 4 Simulation of ultrasonic wave generation

5. Wave Reflection and Mode Conversion

Calculations for wave propagation are carried out using the small wave unit of the ray. The factors of the simulated wave (wave length, velocity, direction, wave mode, and sound pressure) can be contained in this wave unit. The ray is sometimes divided into two rays by refraction or reflection with mode conversion. The sound pressure of a refracted and a reflected wave changed as a function of the refraction or reflection angle. These factors were included in the present simulation. The direction angle of a refracted or a mode-converted wave was calculated by the following equation (Snell's law).

$$V_L / V_S = \sin\theta_L / \sin\theta_S \tag{4}$$

where

V_L is longitudinal wave velocity;

V_S is shear wave velocity;

θ_L is longitudinal wave angle;

θ_S is shear wave angle.

In this simulation, the wave velocity of the

longitudinal wave and the shear wave in pyrex glass specimen were taken as 5940 and 3420 m/s, respectively. The density of pyrex glass was 2119 kg/m^3.

Since longitudinal waves propagate faster than shear waves, the extension step of the longitudinal wave unit is set as V_L/V_S times the length of the shear wave unit in simulation. An example of reflection and ray division by mode conversion is presented in Fig. 5. Number 1 ray is a shear wave that propagates and reflects twice, with no mode conversion. Number 2 ray is a shear wave that is converted into a longitudinal mode at the second reflection and reconverted into a shear wave at the third reflection. At the first reflection, mode conversion does not occur because of the large incident angle to the bottom surface. Number 3 ray shows a mode-converted longitudinal wave. Such reflection and ray divisions by mode conversion were calculated for all rays in simulation.

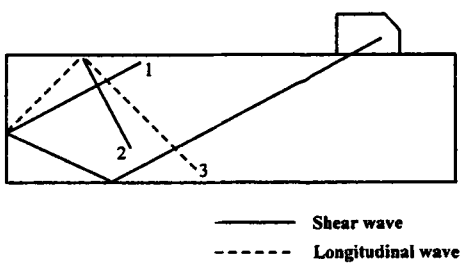

Fig. 5 Simulation of ultrasonic wave propagation, reflection, and mode conversion

The change of the sound pressure values by reflection and mode conversion of rays was calculated using the reflection coefficient, where the initial sound pressure values of the wave unit were taken as "1". The mode-converted wave unit was given the reflection coefficient as its sound pressure. The sound pressure value in the wave unit was used for the calculation of directivity and for the echo analysis. The incident angle relative to the boundary is determined as the angle between the wave propagation direction and the normal direction to the boundary at the reflection point.

6. Discussion

A pyrex glass specimen, shown in Fig. 6, was used to investigate the validity of this simulation method. The thickness of the specimens was 20 mm. It was the model of a butt joint with a round weld reinforcement and a surface-breaking crack.

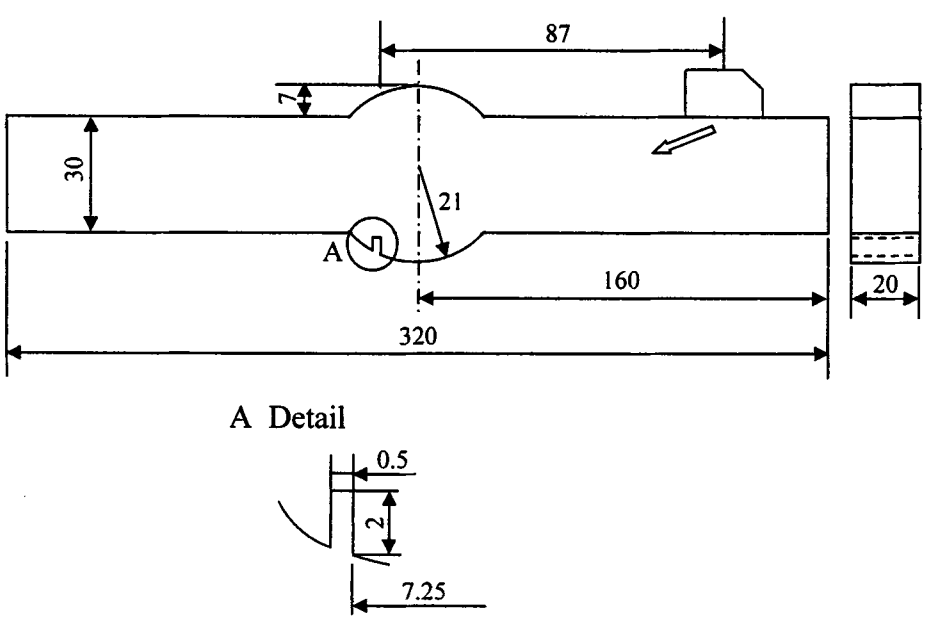

Fig. 6 Dimension of test specimen

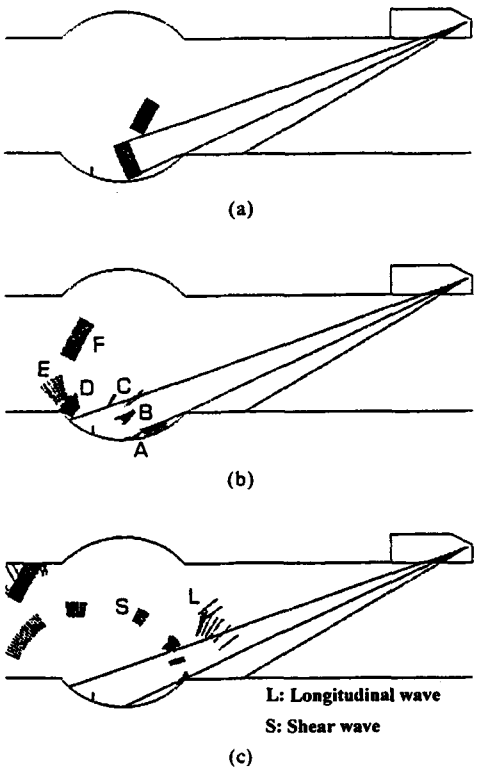

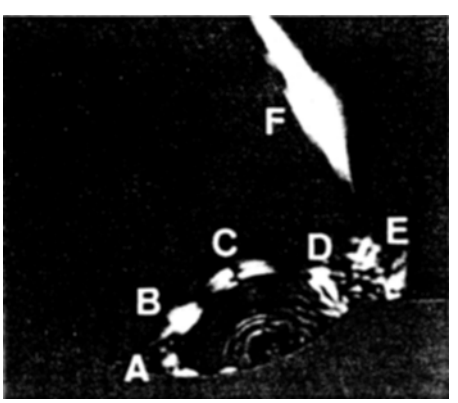

(d)

Fig. 7 Simulation (a~c) of wave propagation and visualization image (d)

The probe position was located 87 mm away from the crack, where the maximum amplitude of the crack echo was observed in ultrasonic testing of this pyrex glass model.

Figure 7(a), (b), and (c) show the simulation results of ultrasonic wave propagation through the butt joint model.

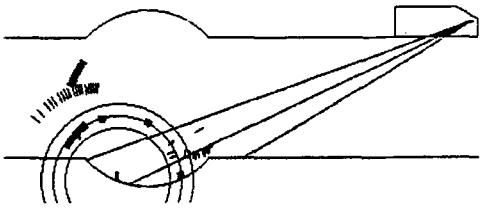

(a) Waves for directivity measurement

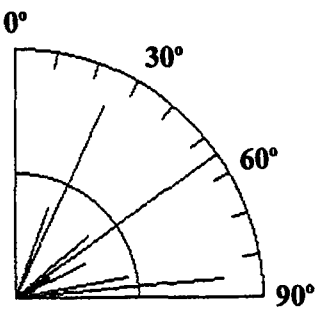

(b) Directivity

Fig. 8 Scattering pattern of simulated wave from a flaw

Actual ultrasonic wave reflection through the pyrex glass model was visualized as shown in Fig. 7(d). Figure 7(d) is reversed horizontally with respect to other figures. The groups of wave units represent the wavefront by showing the same time steps from the source. The mode-converted longitudinal waves are marked L. Comparison of Fig. 7(b) with Fig. 7(d) shows that the simulation of wave propagation in the specimen and the directivity of the reflected waves (A, B, C, D, and E) at the surface-breaking crack agreed with the experimental visualization.

The scattering pattern of waves at the flaw was examined in Fig. 8(a). The center point of the directivity was set at the root corner of the slit defect, and the total sound pressure values of reflected wave units within the circles were calculated every 5 degrees. As shown in Fig. 8(b), the simulated reflection waves propagate in three directions: 25, 55, and 85 degrees.

The simulation results of various echo paths are shown in Fig. 9(a). The simulated A-scan display is shown in Fig. 9(b). Large three echoes were obtained at about 97, 113, and 135 mm beam path distances in this simulation. Mode con-

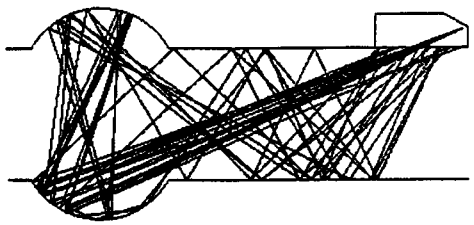

(a) Various paths of echoes

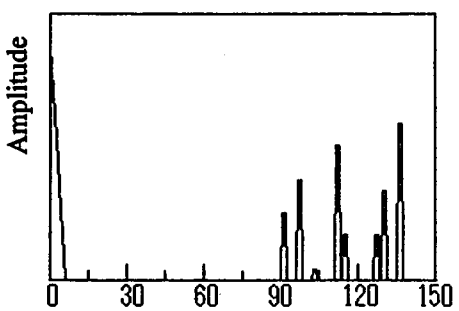

(b) Simulated A-Scan

Fig. 9 A-scan display of butt joint model

version is considered in Fig. 9(a). All waves that returned to the probe were taken as echoes. Some echoes that reflected at the surface-breaking crack were regarded as crack echoes, and the others spurious echoes. The time of each echo on the A-scan display was calculated using the arrival time of the wave unit along the ray. The amplitudes of echoes on the A-scan display were obtained from the summation of the sound pressure value of the wave units returning to the probe at the same time step. By examining each echo path in this simulation, it was determined that the 95 mm echo was from the crack, and the 110 and 130 mm echoes were the spurious echoes. The amplitudes of the echoes are slightly different from the simulation results because there is a sensitivity difference due to the incident angles of the echo to the probe and the wave mode, shear or longitudinal.

From these results, the path of ultrasonic waves in the specimen and the echo position in an A-scan display can be predicted by using the simple model of ultrasonic testing.

7. Conclusions

A simple model has been developed which allows for the tracing of ultrasonic rays within a butt welded joint. Potential applications of this model have been described.

In practice, weld structures will vary from the idealized structures used here, so, some refinements must be added for accuracy. Nevertheless, this simplified model reveals a number of interesting details about ultrasonic testing. This means that the model can be used to optimize the parameters of a testing system.

We intend in a future work to produce more results by treating the austenite as an inhomogeneous material, with a grain structure which varies throughout the weld. In this case, the effects of beam distortion on passing through the austenite will also be included. It is hoped, however, that the results presented here will draw attention to the necessity of such studies for reliable ultrasonic testing.

References

Baborovsky, V.M., Marsh, D.M., Slater, E.A., 1973, "Schlieren and Computer Studies of the Interaction of Ultrasound with Defects," *British Journal of NDT*, pp. 200~207

Harker, A.H., 1984, "Numerical Modeling of the Scattering of Elastic Waves in Plates," *Journal of Nondestructive Evaluation*, pp. 89~106.

Harumi, K., 1986, "Computer Simulation of Ultrasonic in a Solid," *NDT & E International*, pp. 315~332.

Harumi, K., and Uchida, M., 1990, "Computer Simulation of Ultrasonic and Its Applications," *Journal of Nondestructive Evaluation*, pp. 81~99.

Harumi, K., Uchida, M., Miyajima, T., and Ogura, Y., 1992, "Defect Sizing of Small Inclined Cracks on a Free Surface Using Multi-Tip Waves," *NDT & E International*, pp. 135~143.

Nam, Y.H., 1999, "Directivity Analysis of Ultrasonic Waves on Surface Defects Using a Visualization Method," *KSME International Journal*, pp. 158~167.

Nam, Y.H., 1999, "Directivity Evaluation of an Artificial Defect in a Simulated Butt Joint by the Visualization Method," *Welding Journal*, pp. 338~342.

Ogilvy, J.A., and Temple, J.A. G., 1983, "Diffraction of Elastic Waves by Cracks: Application to Time-of-Flight Inspection," *Ultrasonics*, pp. 259~269.

Ogilvy, J. A., 1984, "Identification of Pulse-Echo Rays in Austenitic Steels," *NDT International*, pp. 259~264.

Ogilvy, J.A., 1985, "Computerized Ultrasonic Ray Tracing in Austenitic Steel," *NDT International*, pp. 67~77.

Ogilvy, J.A., 1986, "Ultrasonic Beam Profiles and Beam Propagation in an Austenitic Weld Using a Theoretical Ray Tracing Model," *Ultrasonic*, pp. 337~347.

Ogilvy, J.A., 1987, "On the Use of Focused Beams in Austenitic Welds," *British Journal of NDT*, pp. 238~246.

Ogilvy, J.A., 1988, "Ultrasonic Reflection Properties of Planar Defects Within Austenitic Welds," *Ultrasonics*, pp. 318~327.

Ogilvy, J.A., 1992, "An Interactive Ray Tracing Model for Ultrasonic Nondestructive Testing," *NDT International*, pp. 3~10.

Serabian, S., 1982, "Ultrasonic Probability of Detection of Subsurface Flaws," *Materials Evaluation*, pp. 294~298.